A System Level Simulator for Reliable Smart Energy Networks

S. Tennina*, D. Xenakis†, M. Boschi*, A. Colarieti*, N. Passas†, D. Tsolkas† and P. Vezinias‡
*WEST Aquila S.r.l., L'Aquila, Italy
{tennina, mattia.boschi, andrea.colarieti} at westaquila.com
†Department of Informatics and Telecommunications, University of Athens, Greece,
{nio, passas, dtsolkas} at di.uoa.gr
‡LINK Technologies S.A., Thessaloniki, Greece
makis at link-tech.gr

***Abstract*—Power grids are deployed and used worldwide and served well in providing a seamless unidirectional power supply of electricity. However, today a new set of challenges is arising, such as the depletion of primary energy resources, the diversification of energy generation and the climate change. With this regard, Smart-NRG project aims to propose new technologies to meet the specific requirements of smart grids applications by proposing a modular and flexible system architecture to face with the challenges imposed by the different application scenarios. In particular, in this paper, we present the simulator developed to implement such a system architecture. Our results demonstrate that adopting cooperative communications among the smart meters in the network is paramount to achieve good performance. This is evident for the end-to-end data reliability, while, provided that the network connectivity is sufficiently high, even a simple binary XOR-based network coding technique is enough to allow gains in terms of network throughput.**

I. Introduction

Today a new set of challenges is arising for power grids, such as the depletion of primary energy resources, the diversification of energy generation, and the climate change [1]. Therefore, the existing power grid is evolving into a more responsive and more efficient system, known as the Smart Grid (SG) [2]. To fully exploit the power of such new paradigm, efficient, reliable and secure two-way information flow among the customers and the utility companies is mandatory. In this perspective, the electricity meters are evolving into a new generation of devices with the necessary intelligence to enable such two-way communications, since they are capable of collecting and delivering actual power consumption reports to remote utilities, more efficiently than conventional meters [3]. Utility companies are then able to setup Smart Energy Networks (SENs) to better monitor the energy consumption, using appropriate energy algorithms [4] and communication protocols [5]. For instance, in a home environment, the smart meter collects the power consumption information of the dishwasher, TV and the refrigerator, and also sends the control commands to them, if necessary. The data generated by the smart meters in different buildings is transmitted to a data aggregator (i.e., an access point or gateway), which collects measurements and may take the appropriate control actions locally for cost optimizations or can report them to a remote electric utility.

Three functionalities are instrumental for the long-term success of SENs: (*i*) Efficient and reliable networking protocols, to enable two-way communications between the smart meters and the utility companies. (*ii*) Robust and real-time smart energy/management algorithms. (*iii*) Secure and trusted mechanisms and algorithms. Accordingly, SENs can be regarded as an electric system, which uses two-way networking technologies, cyber-secure communications technologies, computational intelligence and control in an integrated fashion, with the aim of providing a new way of electricity distribution that is safer, secure, reliable, efficient and sustainable.

Moving from the system architecture already identified in [6] and briefly recalled in next section, in this paper we aim to present the System Level Simulator (SLS) developed in the frame of our Smart-NRG project [7], along with preliminary results in different simulation scenarios to show how the potential benefits of SENs can be achieved. Accordingly, the remaining of this paper is organized as follows. Section II recalls the system architecture scheme already introduced in [6]. Section III overviews the SLS, while Section IV presents the simulation setup and discuss the results achieved. Finally, Section V concludes the paper.

II. System Architecture

The current trend for modeling SG-specific architectures is the adoption of multi-layer and heterogeneous architectures for the SG communication infrastructure [8]. Such a layering approach enables the network engineers to reduce computing, memory and system complexity requirements for the intermediate nodes, to aggregate control/metering traffic, prioritize emergency messages, and also utilize data fusion and aggregation techniques.

Accordingly, the main technologies for the communication system that constitutes the reference architecture for Smart-NRG are depicted in Figure 1. In particular, short range communication technologies (e.g., ZigBee/IEEE 802.15.4) are used in home and office indoor environments, with the goal of reaching the smart meter from every electrical equipment with the least number of intermediate hops to minimize the communication delays. Then, to reinforce the reliability of the system, a wireless mesh based network is built among the smart meters to reach the access point for medium-long range communications (e.g., WLAN/IEEE 802.11). At the level of the microgrid, the mesh network intrinsically ensures that in

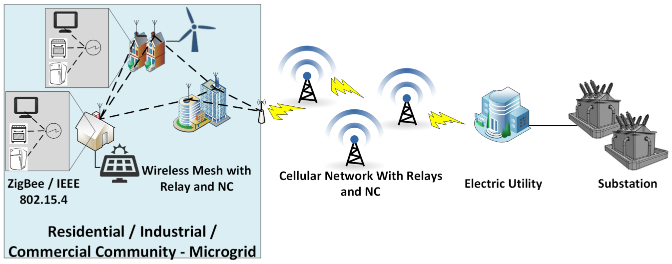

Figure 1. An example of the Smart-NRG system (inspired by [4]).

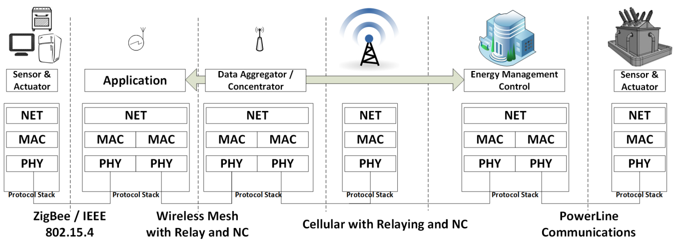

Figure 2. Communication Protocol Architecture.

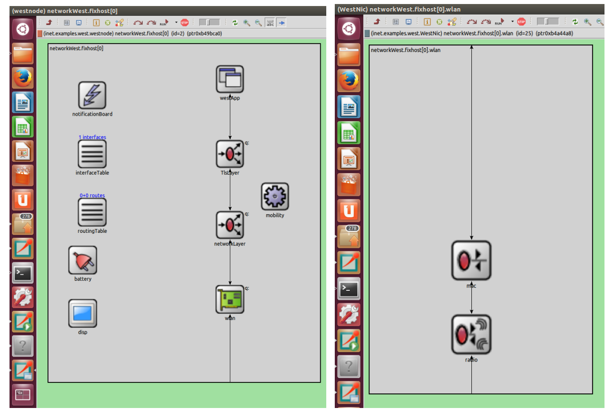

Figure 3. Network node in the simulator. (left) Protocol Stack is composed by three layers on top of the Network Interface: *NET*, *TLS* and *APP*. (right) Network Interface is composed by *MAC* and *PHY* layers.

the case of nodes or links faults, the presence of multi-path guarantees that information is delivered from the source(s) to the access point, which will play the role of data aggregator. Then, long range communications (e.g., cellular and LTE based networks) implement the two-ways connection of the microgrid with the electric utility (and then the substation).

The adoption of cooperative communications schemes, through Relay-aided and Network Coding (NC) [9], at the level of both the mesh microgrid and the long range networks is paramount to helps improving reliability and scalability of the system. Figure 2 sketches the composition of these communication protocol stacks into the full picture of the system architecture, as developed in our SLS and detailed in Section III.

III. System Level Simulator

The SLS developed in the frame of the Smart-NRG project is built upon the OMNeT++ framework [10], i.e., a discrete event network simulator environment. The simulated network represents the structure of a microgrid as by the architecture recalled in Figure 1 and is composed by three kind of devices communicating with each other through wireless links: (*i*) End Device (ED): it is the sensor node which collects measurements to be passed to the smart meter. (*ii*) Smart Meter (SM): it collects the measurements generated by the EDs that it coordinates, and forwards them to the aggregator. (*iii*) Aggregator: it is where all the measurements are collected and processed for taking eventually any intervention.

Figure 3 shows the composition of the protocol stack of the generic node into a total of 5 layers which are summarized next. (*i*) **APP**: It is a traffic generator and where measurements are collected. For the EDs a packet representing the measurements is periodically generated and sent down every $timeGenerationInterval$ seconds. On the SMs the measurements arrived from the EDs are collected into a single report and sent towards the Aggregator. On the Aggregator the information about the packets received are logged onto a file for later performance analysis. (*ii*) **TLS**: it is a layer where data are expected to be protected through some security mechanism (ciphering, cryptography and so on). This layer implements some basic mechanism, but they are not enabled for the purposes of this paper. As such, raw packets pass through this layer in both directions (downwards, from *APP* to *NET*, and upwards, from *NET* to *APP*). (*iii*) **NET**: it is the layer responsible to route packets from sources to destination. It implements a Tree- and Geographical-based routing protocol. The logical topology of the SMs' network is assumed to be a tree rooted at the Aggregator node and each node knows its own position and the position of the Aggregator. The EDs form a star network with their own coordinator SM and the two networks (SM-EDs and SMs-SMs-Aggregator) runs in parallel on distinct frequency channels. The nodes are supposed to have a unique address and at this layer the communications for the measurements reporting are unicast, i.e., a node can send its packet to only one recipient. Finally, this layer is responsible to relay the packets from SMs to the Aggregator and can optionally perform network coding on the packets in transit. The relay and network coding procedures will be described next in Section III-B. (*iv*) **MAC**: it is the layer inside the Network Interface responsible to access the wireless medium. It implements a Time Division Multiple Access (TDMA) protocol and, as such, collisions are avoided a priori. To enable network coding at the *NET* layer, the transmissions at the *MAC* layer are always in broadcast (i.e., MAC frames are received by all nodes in the transmission range). (*v*) **PHY**: it is the layer inside the Network Interface responsible to handle the transmission and reception of frames over the wireless medium. In the simulation, two PHYs are implemented: one IEEE 802.15.4-like [11] for the EDs and another IEEE 802.11-like [12] for the Aggregator, while the SMs have both. For the sake of simplicity, in the current implementation of the simulator we opted to use the simpler unit-disk model, i.e., the radio coverage of a node is defined by its transmission range and every node inside the transmission range of a sender receives sender's frames. Then, to recover realism, a Packet Reception Ratio (PRR) model has been implemented as described next in Section III-A.

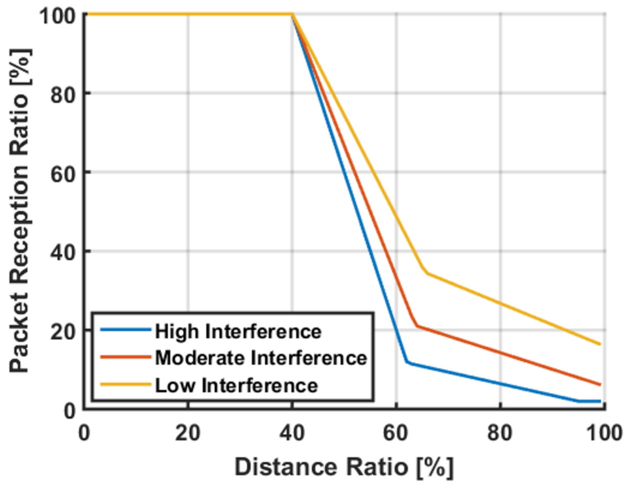

Figure 4. Packet Reception Ratio vs. Distance Ratio model for the different interference scenarios.

A. *Packet Reception Ratio Model*

In order to include the effects of different interference levels into the SLS, we opted to implement a model inspired by [13], [14], which correlates the PRR to the distance separating the transmitter's from the receiver's antennas. Figure 4 shows such a model. First we define the Distance Ratio as the normalized distance between the transmitter and the receiver of an incoming transmission, where the normalization is done with respect to the transmission range. Then, three interference scenarios have been simulated, as a gradient ranging from Low to High interference, with different packet reception probabilities (Figure 4).

Accordingly, when a frame is received at the *MAC* layer of a node from the *PHY* layer, the node computes the probability to lose the packet: it guesses from a random uniform variable and compares it with the threshold given by the model. If the local random guess is lower than the threshold at the given distance ratio and interference scenario, then the frame is discarded, otherwise it is handled and the data contained in it are passed up to the *NET* layer.

B. *Relay Only and Network Coding Mechanisms*

When the *NET* layer receives a data packet from the upper layer to be sent to the destination, two cases are handled: (*i*) For the EDs: the data contain sensor measurements, thus both the destination and the next stop are set as the parent SM. (*ii*) For the SMs: the data contain an aggregated measurement report and the destination is set to the Aggregator, while the next stop is computed locally by the *NET* layer as the neighbour node to which address the packet.

On the other hands, Figure 5 illustrates the behavior of the SMs nodes when the *NET* layer receives the data packet from the *MAC* layer, and is detailed as follows. If the current node is the final destination, it passes the encapsulated data contained in the packet to the upper *TLS* layer. This is the case when the node is a SM receiving measurements from its local EDs, or the Aggregator node, which is receiving aggregated reports from the SMs.

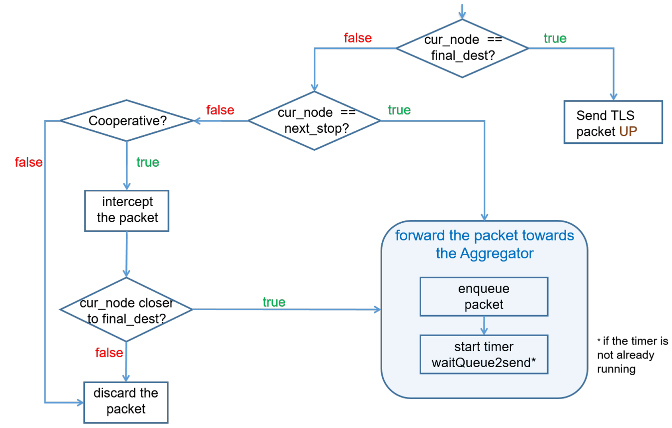

Figure 5. Routing policy at the *NET* layer when a packet is received from the *MAC* layer.

If the current node is not the final destination, the node is a SM and there are two cases: (*i*) If the node is the intended next stop, it needs to forward the packet towards the Aggregator. It enqueues the packet and starts a waiting timer (for *waitQueue2send* seconds) to elaborate the queue, if the timer is not already running. (*ii*) If the node is not the next stop, it simply discards the packet in the *non-cooperative* scenario, or intercepts the packet to generate useful redundancy in the *cooperative scenarios*. In the latter case, if the node is closer to the final destination (i.e., the Aggregator) than the node from which the packet has been just received, it enqueues the packet in the same queue as in the case above and start the timer, if not already scheduled. Otherwise, in the case where the node is farther away from the Aggregator than the packet's sender, it just discards the packet. This geographical-based on-line packet filtering policy reflects the fact that, whatever the interference scenario is, the probability of loosing a packet is directly proportional to the distance separating the transmitter from the receiver; thus the tentative is to allow the intermediate relay nodes to generate only potentially useful redundancy.

When the waiting timer expires, for the *cooperative* scenario there are two cases: (*i*) In the relay only scenario, the SM forwards to its parent every packet present in the queue. (*ii*) In the network coding scenario, the SM tries opportunistically to combine pairs of packets from the queue into one packet by implementing a simple binary NC scheme, i.e., the bitwise XOR on the payloads of two packets, and then sends the new packet to its parent node. The original enqueued packets are then discarded. For the sake of clarity, we recall that the principle of a binary NC scheme leverages on the fact that given $C = xor(A, B)$ and assumed that a node D receives A and C and looses B, it can recover the missing data in an easy way by computing $B = xor(A, C)$.

The following assumptions hold. (*i*) Each packet has a Time To Live (TTL) value, which is initialized at the first sending and is decreased by one in every transmission by intermediate nodes. If a node receives a packet with TTL equals to zero and it is not the final destination, the packet that should be forwarded is then discarded. (*ii*) In the network coding scenario, the intermediate SM nodes never combine their own packets with the ones they have to relay and (*iii*) if a node receives a packet which is already the combination of two packets by bitwise XOR operation, then the packet is not allowed to be further combined with another one and is simply forwarded. Indeed, the latter assumption quite limits the performance gains and can be removed by adopting more sophisticated network coding algorithms, as e.g., [15].

IV. Simulation Setup and Results

In this section we aim to show results of the networking between the smart meters under a system level perspective within a microgrid, as by the architecture recalled in Figure 1 and implemented into the SLS. A set of simulations has been performed in different scenarios to assess the reliability and performance of the network. Three topologies have been simulated according to the scenarios described early in [6]: (*i*) A network of 7 nodes, i.e., an Aggregator, 3 SMs and one ED per each SM. This network has an average connectivity of 35.7%, i.e., the number of neighbors of each node normalized to the number of nodes. This network represents a microgrid of a dense urban scenario, where it is assumed that a multiplicity of aggregators serve a lower number of smart meters deployed over small areas and this results into a large number of microgrids. (*ii*) A network of 15 nodes, i.e., an Aggregator, 7 SMs and one ED per each SM. This network has an average connectivity of 35.0%. This scenario represents a sparse urban or rural scenario, where the area covered by a single microgrid is slightly larger than the previous case. (*iii*) A network of 25 nodes where the nodes are arranged based on the Cluster Tree Topology with characteristic parameters [16]: $L_m = 3$, $C_m = 4$ and $R_m = 3$, i.e., maximum depth is three hops, where the root Aggregator is at depth 0, up to 4 children nodes per parent and up to three of which are SMs. This network has an average connectivity of 15.4% and represents a larger scale scenario, where the single microgrid should cover a larger area than the previous cases.

For each topology all the three interference scenarios have been considered, as by the referred PRR model described in Section III-A. It is worth mentioning that the last scenario defined in [6], i.e., the industrial scenario, is a particular case, since it covers the different kind of microgrid topologies, but is characterized by the usually high interference. Consequently, the industrial scenario is seen as the high level interference case, spread across the three microgrid topologies.

Finally, three simulation's runs for each interference scenario and network setup have been performed: (*i*) the non cooperative scenario, (*ii*) the relay only and (*iii*) relay with network coding, as described in Section III-B.

In each run, at the *APP* layer, the EDs nodes start generating measurements data and send periodically these packets every *timeGenerationInterval* seconds. As soon as the SM receives the first ED's measurements packet, it starts a timer whose duration is *waitToReport* seconds. When the timer expires, it generates and sends the report. Each time the EDs send their data a new epoch begins. EDs stop generating measurements when *maxNumEpochs* is reached, i.e., they send up to *maxNumEpochs* packets. The main simulation parameters, their values and their meaning are summarized in Table I.

The performance indices considered are the reliability and the goodput measured at the Aggregator node, and they are defined as follows: (*i*) Reliability: the useful SMs' reports arriving at the Aggregator node. It is a value computed for each epoch as: PRR = number of distinct SMs' reports / number of SMs. (*ii*) Goodput: it measures the useful information ratio available at the Aggregator in the unit of time. Since the network is regulated on a strict TDMA basis, under the assumption that a packet is transmitted in one slot, the time is expressed as number of packets. Consequently, in each epoch the goodput is computed as: Goodput = number of distinct SMs' reports / (num packets received at Aggregator + num packets lost at Aggregator).

Table I. Simulation parameters.

Name	Value [Unit]	Meaning
timeGenerationInterval	1 [s]	EDs measurements' generation interval.
maxNumEpochs	1000	Maximum number of ED's packets.
waitToReport	100 [ms]	Timer to wait to generate the report at SM after having received the first measurement from an ED in an epoch.
initTTL	3	Initial time to live value of a packet. It indicates the maximum number of allowed packet's forwarding.
waitQueue2send	300 [ms]	Timer to wait to process the forwarding queue at NET layer after having enqueued the first packet.
txRangeSM	150 [m]	Transmission range for SM to SM IEEE 802.11-like communications.
txRangeED	30 [m]	Transmission range for ED to SM IEEE 802.15.4-like communications.

We report in Figure 6, Figure 7 and Figure 8 the simulation results obtained in the case of the networks formed by 7, 15 and 25 nodes, respectively, and for the three interference patterns defined in Figure 4. More in details, Figure 6(a), Figure 7(a) and Figure 8(a) show the average PRR measured at the Aggregator node in different epochs, while Figure 6(b), Figure 7(b) and Figure 8(b) illustrate the traces of the average goodput, yet measured at the Aggregator node, with respect to the different epochs. As it is evident, the cooperative behavior of neighbor nodes greatly helps in achieving better performance in terms of PRR at the Aggregator node, regardless of the specific interference pattern or scenario. More in details, the relay-only behavior is slightly outperforming the network coding approach, when the network connectivity decreases. On the other hands, in terms of goodput, the results demonstrates that the non-cooperative approach has the better performance, since it lacks of redundant packets. The comparison between the network coding approach and the relay-only shows that the former slightly outperforms the latter one for low and moderate interference, provided that a sufficient network connectivity level is available. This is because combining packets helps keeping the redundancy level at the Aggregator low.

Table II provides a summary of the numeric results and helps getting the overall picture. With respect to the scenarios defined in [6], we highlight the following results: (*i*) For a dense urban scenario, the relay-only solution performs as good as the NC in terms of packet delivery ratio and goodput at the destination. (*ii*) For a rural scenario, the relay-only solution performs slightly better than the NC in terms of packet delivery ratio at the destination, since the loss of a combined packet leads to a loss of more information, however this is paid by a loss in terms of goodput ranging from 1.1% up to 4.4%. (*iii*) For a large scale scenario: the low connectivity impacts on the benefit of the NC given that the relay-only scenario shows better performance in terms of both reliability and goodput.

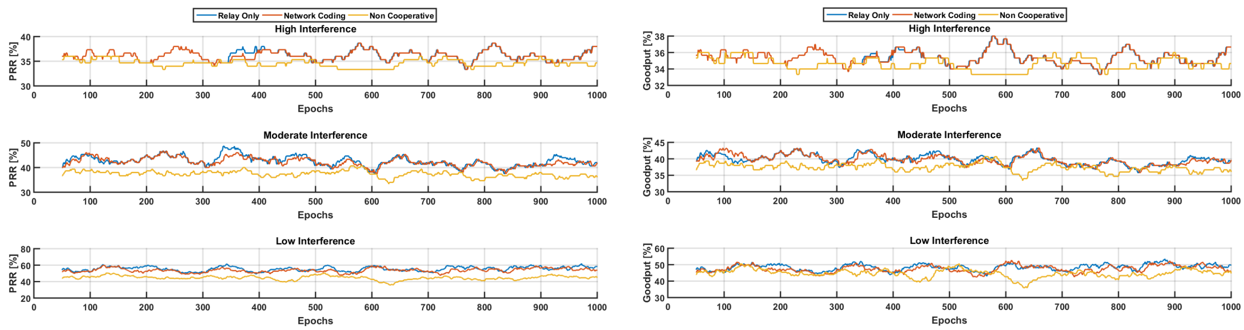

(a) Reliability as Packet Reception Ratio measured at the Aggregator node.

(b) Goodput measured at the Aggregator node.

Figure 6. Simulation results for the 7 nodes multihop network in the three interference scenarios. This network has an average connectivity of 35.7%. The traces are the moving average over the time using a window's size of 50 epochs.

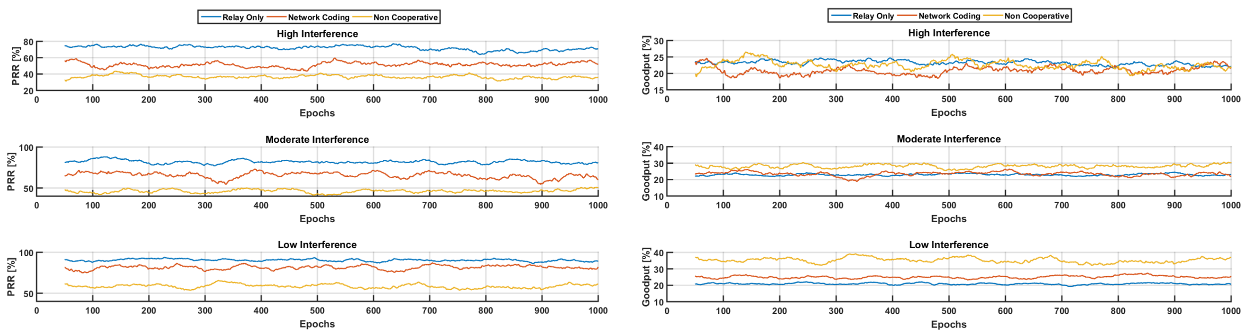

(a) Reliability as Packet Reception Ratio measured at the Aggregator node.

(b) Goodput measured at the Aggregator node.

Figure 7. Simulation results for the 15 nodes multihop network in the three interference scenarios. This network has an average connectivity of 35.0%. The traces are the moving average over the time using a window's size of 50 epochs.

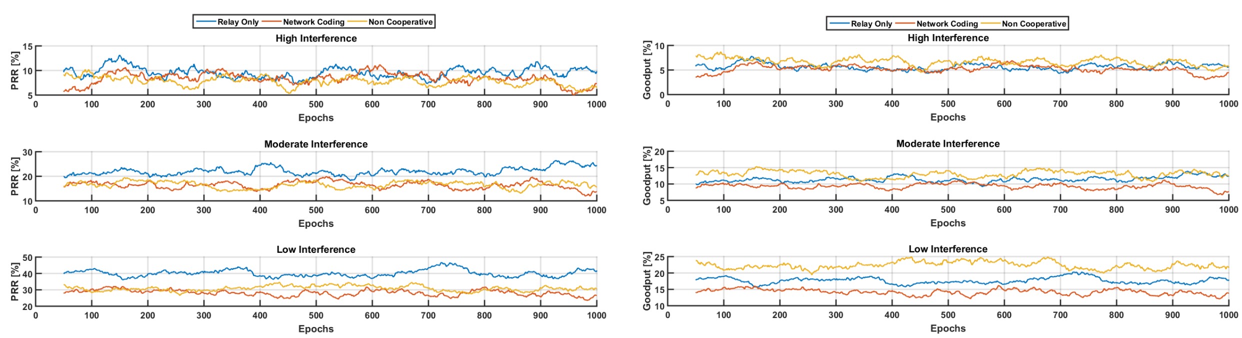

(a) Reliability as Packet Reception Ratio measured at the Aggregator node.

(b) Goodput measured at the Aggregator node.

Figure 8. Simulation results for the 25 nodes multihop network in the three interference scenarios. This network has an average connectivity of 15.4%. The traces are the moving average over the time using a window's size of 50 epochs.

(*iv*) For the industrial scenario, given by looking at the high interference cases of the three topologies, it is shown that the packet delivery ratio and goodput at the destination of the relay-only solution is similar to the performance of the NC, except in the case of medium size microgrids, where the relay-only can deliver an average of 14.3% packets more than the NC, but this is paid by an effort in terms of goodput, since the relay-only differs from the NC of -2%.

Overall, it is worth stressing that, only for the scenarios where the network connectivity is relatively high (the dense urban and the rural cases, characterized by an average connectivity of 35.7% and 35.0%, respectively, in contrast with the large scale network, having a connectivity of only 15.4%), the Network Coding approach is able to achieve gains in terms of goodput at the Aggregator node, with some sensitive differences in terms of reliability.

V. Conclusion

In this paper we briefly recalled the modular and flexible architecture we have identified in the frame of our Smart-NRG project, then we have presented the system level simulator built upon OMNET++ and developed to address performance

Table II. SUMMARY OF THE SIMULATION RESULTS. (A) REFERS TO RELAY ONLY, (B) REFERS TO NETWORK CODING, (C) REFERS TO NON-COOPERATIVE.

Scenario		PRR avg [%]	PRR std [%]	PRR min [%]	PRR max [%]	Goodput avg [%]	Goodput std [%]	Goodput min [%]	Goodput max [%]
Dense Urban	*Low Interference*	a) 66.6 b) 66.6 c) 33.3	a) 22.3 b) 21.6 c) 17.5	a) 33.3 b) 33.3 c) 33.3	a) 100 b) 100 c) 100	a) 50 b) 50 c) 33.3	a) 16.3 b) 16.6 c) 17.5	a) 33.3 b) 25 c) 33.3	a) 100 b) 100 c) 100
	Moderate Interference	a) 33.3 b) 33.3 c) 33.3	a) 16.5 b) 15.7 c) 11.4	a) 33.3 b) 33.3 c) 33.3	a) 100 b) 100 c) 100	a) 33.3 b) 33.3 c) 33.3	a) 12.1 b) 12.3 c) 11.4	a) 33.3 b) 25 c) 33.3	a) 100 b) 100 c) 100
Rural	*Low Interference*	a) 85.7 b) 85.7 c) 57.1	a) 10.9 b) 19 c) 17	a) 42.8 b) 14.3 c) 14.3	a) 100 b) 100 c) 100	a) 20.6 b) 25 c) 33.3	a) 3.6 b) 6.1 c) 10.1	a) 9.4 b) 4.3 c) 8.3	a) 36.8 b) 46.7 c) 60
	Moderate Interference	a) 85.7 b) 71.4 c) 42.8	a) 14.2 b) 24.1 c) 16.9	a) 28.6 b) 0 c) 0	a) 100 b) 100 c) 100	a) 22.7 b) 23.8 c) 27.3	a) 4.4 b) 8.4 c) 10.1	a) 9.1 b) 0 c) 0	a) 41.2 b) 46.7 c) 58.3
Large Scale	*Low Interference*	a) 41.7 b) 25 c) 33.3	a) 13.8 b) 12.1 c) 12.7	a) 8.3 b) 0 c) 0	a) 91.7 b) 75 c) 75	a) 17.6 b) 13.6 c) 22.2	a) 5.7 b) 5.9 c) 8.5	a) 3.3 b) 0 c) 0	a) 35.5 b) 36 c) 50
	Moderate Interference	a) 25 b) 16.7 c) 16.7	a) 11.5 b) 10 c) 10.4	a) 0 b) 0 c) 0	a) 58.3 b) 50 c) 50	a) 11.1 b) 9.1 c) 13.3	a) 5.8 b) 5.6 c) 7.9	a) 0 b) 0 c) 0	a) 31.6 b) 27.8 c) 37.5
Industrial (High Interference)	*Small-size microgrid*	a) 33.3 b) 33.3 c) 33.3	a) 9.6 b) 9.3 c) 6.5	a) 33.3 b) 33.3 c) 33.3	a) 100 b) 66.6 c) 100	a) 33.3 b) 33.3 c) 33.3	a) 7.2 b) 7.3 c) 6.5	a) 33.3 b) 25 c) 33.3	a) 66.6 b) 66.6 c) 100
	Medium-size microgrid	a) 71.4 b) 57.1 c) 42.8	a) 16.3 b) 24 c) 16.7	a) 14.3 b) 0 c) 0	a) 100 b) 100 c) 85.7	a) 23 b) 21 c) 25	a) 5.2 b) 9.5 c) 10.2	a) 4.3 b) 0 c) 0	a) 40 b) 50 c) 55.5
	Large microgrid	a) 8.3 b) 8.3 c) 8.3	a) 8.1 b) 7.9 c) 7.2	a) 0 b) 0 c) 0	a) 41.7 b) 33.3 c) 41.7	a) 5 b) 5 c) 7.1	a) 4.7 b) 4.9 c) 6.1	a) 0 b) 0 c) 0	a) 26.3 b) 22.2 c) 33.3

assessment. This tool has been improved to include at the *NET* layer a simple binary XOR-based network coding technique, based on which smart meters are able to opportunistically combine pairs of packets in a full cooperative fashion, to improve the overall network throughput. Notably, the results confirmed that the cooperative behavior of the network is diriment to achieve higher reliability. In fact, results demonstrated that cooperation attains a gain of up to 42.9% in terms of packet reception ratio when compared with the non-cooperative behavior. Moreover, results show that even the simplest binary NC technique is enough to gains in terms of goodput with respect to the relay-only case, if the network connectivity is sufficiently high. These gains might be amplified if proper relay selection mechanisms and random linear network coding approaches [15] will be adopted, since they allow for combining multiple packets, instead of just pairs of them.

ACKNOWLEDGEMENT

This research has been funded by the European Commission as part of the Smart-NRG project (FP7-PEOPLE-2013-IAPP Grant number 612294).

REFERENCES

[1] C. H. Hauser et al., "Security, trust, and qos in next-generation control and communication for large power systems," *Int. J. of Critical Infrastructures*, vol. 4, no. 1, pp. 3–16, 2008.

[2] V. C. Gungor et al., "Smart grid technologies: communication technologies and standards," *IEEE TII*, vol. 7, no. 4, pp. 529–539, 2011.

[3] N. Kayastha et al., "Smart grid sensor data collection, communication, and networking: a tutorial," *Wireless comm. and mobile comp.*, vol. 14, no. 11, pp. 1055–1087, 2014.

[4] X. Fang et al., "Smart gridthe new and improved power grid: A survey," *IEEE Comm. Surveys & Tutorials*, vol. 14, no. 4, pp. 944–980, 2012.

[5] M. Carlesso et al., "Uplink scheduling for smart metering and real-time traffic coexistence in LTE networks," in *2015 IEEE ICC*, June 2015, pp. 820–825.

[6] S. Tennina et al., *Ad-hoc, Mobile, and Wireless Networks: 14th International Conference, ADHOC-NOW 2015, Athens, Greece, June 29 – July 1, 2015, Proceedings*. Cham: Springer International Publishing, 2015, ch. A Modular and Flexible Network Architecture for Smart Grids, pp. 273–287. [Online]. Available: http://dx.doi.org/10.1007/978-3-319-19662-6_19

[7] (2014) Smart-nrg: An industry-academia partnerships and pathways for smart energy networks. Http://gain.di.uoa.gr/smart-nrg. [Online]. Available: http://gain.di.uoa.gr/smart-nrg

[8] H. Gharavi and B. Hu, "Multigate communication network for smart grid," *Proc. of the IEEE*, vol. 99, no. 6, pp. 1028–1045, 2011.

[9] R. Ahlswede et al., "Network information flow," *IEEE Trans. on Inf. Theory*, vol. 46, no. 4, pp. 1204–1216, 2000.

[10] (2015) Omnet++ 4.x discrete event simulator. Www.omnetpp.org. [Online]. Available: www.omnetpp.org

[11] IEEE, "Standard for information technology - local and metropolitan area networks - specific requirements - part 15.4: Wireless medium access control (MAC) and physical layer (PHY) specifications for low rate wireless personal area networks (WPANs)," *IEEE Std 802.15.4-2006 (Revision of IEEE Std 802.15.4-2003)*, pp. 1–320, Sep. 2006.

[12] ——, "Standard for information technology–telecommunications and information exchange between systems local and metropolitan area networks–specific requirements part 11: Wireless LAN medium access control (MAC) and physical layer (PHY) specifications," *IEEE Std 802.11-2012 (Revision of IEEE Std 802.11-2007)*, pp. 1–2793, March 2012.

[13] M. R. Souryal et al., "Link assessment in an indoor 802.11 network," in *IEEE WCNC*, vol. 3, April 2006, pp. 1402–1407.

[14] N. Baccour et al., "Radio link quality estimation in wireless sensor networks: A survey," *ACM Trans. Sen. Netw.*, vol. 8, no. 4, pp. 34:1–34:33, Sep. 2012. [Online]. Available: http://doi.acm.org/10.1145/2240116.2240123

[15] A. Antonopoulos et al., "Cross-layer theoretical analysis of NC-aided cooperative ARQ protocols in correlated shadowed environments," *IEEE Trans. on Vehic. Tech.*, vol. PP, no. 99, pp. 1–1, 2014.

[16] S. Tennina et al., *IEEE 802.15.4 and ZigBee as Enabling Technologies for Low-Power Wireless Systems with Quality-of-Service Constraints*. SpringerBriefs in Electrical and Computer Engineering, 2013, p. 464, iSBN: 978-3-642-37367-1.